Article

In Silico Transcriptomic Analysis of Wound-Healing-Associated Genes in Malignant Pleural Mesothelioma

Erasmia Rouka [1,2], Eleftherios Beltsios [2], Dimos Goundaroulis [3,4], Georgios D. Vavougios [5], Evgeniy I. Solenov [6,7], Chrissi Hatzoglou [2,8], Konstantinos I. Gourgoulianis [8] and Sotirios G. Zarogiannis [2,8,*]

[1]   Department of Transfusion Medicine, Faculty of Medicine, University of Thessaly, BIOPOLIS, 41500 Larissa, Greece; errouka@uth.gr
[2]   Department of Physiology, Faculty of Medicine, University of Thessaly, BIOPOLIS, 41500 Larissa, Greece; elbeltsios@uth.gr (E.B.); chatz@med.uth.gr (C.H.)
[3]   Center for Integrative Genomics, University of Lausanne, 1015 Lausanne, Switzerland; Dimoklis.Gkountaroulis@unil.ch
[4]   Swiss Institute of Bioinformatics, 1015 Lausanne, Switzerland
[5]   Department of Neurology, Athens Naval Hospital, 11521 Athina, Greece; gvavou@uth.gr
[6]   Institute of Cytology and Genetics of the Siberian Branch of the Russian Academy of Sciences, Novosibirsk 630090, Russia
[7]   Novosibirsk State University, Novosibirsk 630090, Russia; eugsol@bionet.nsc.ru
[8]   Department of Respiratory Medicine, Faculty of Medicine, University of Thessaly, BIOPOLIS, 41500 Larissa, Greece; kgourg@med.uth.gr
*   Correspondence: szarog@med.uth.gr; Tel.: +30-2410-685558

check for updates

Abstract: *Background and objectives:* Malignant pleural mesothelioma (MPM) is a devastating malignancy with poor prognosis. Reliable biomarkers for MPM diagnosis, monitoring, and prognosis are needed. The aim of this study was to identify genes associated with wound healing processes whose expression could serve as a prognostic factor in MPM patients. *Materials and Methods:* We used data mining techniques and transcriptomic analysis so as to assess the differential transcriptional expression of wound-healing-associated genes in MPM. Moreover, we investigated the potential prognostic value as well as the functional enrichments of gene ontologies relative to microRNAs (miRNAs) of the significantly differentially expressed wound-healing-related genes in MPM. *Results:* Out of the 82 wound-healing-associated genes analyzed, 30 were found significantly deregulated in MPM. Kaplan–Meier analysis revealed that low *ITGAV* gene expression could serve as a prognostic factor favoring survival of MPM patients. Finally, gene ontology annotation enrichment analysis pointed to the members of the hsa-miR-143, hsa-miR-223, and the hsa-miR-29 miRNA family members as important regulators of the deregulated wound healing genes. *Conclusions:* 30 wound-healing-related genes were significantly deregulated in MPM, which are potential targets of hsa-miR-143, hsa-miR-223, and the hsa-miR-29 miRNA family members. Out of those genes, ITGAV gene expression was a prognostic factor of overall survival in MPM. Our results highlight the role of impaired tissue repair in MPM development and should be further validated experimentally.

Keywords: in silico; malignant pleural mesothelioma; miRNA; transcriptomics; wound healing

1. Introduction

Malignant pleural mesothelioma (MPM) is a highly aggressive tumor of the pleural mesothelium, a metabolically active cell monolayer covering the lungs and the chest wall [1]. Neoplastic

transformation of pleural mesothelial cells (PMCs) develops in the course of asbestos-induced chronic inflammation while genetic susceptibility factors, radiation exposure, and SV40 infection have also been indicated as co-factors in this process [2,3]. Recent evidence from animal studies and a few case series show that engineered nanoparticles, whose use is constantly expanding, can lead to a pathology similar to MPM and, thus, potentially lead to an increase of MPM incidence in the future and the same is the case with air pollution, which has been shown to lead to lung cancer [4,5].

Diagnosis of MPM is challenging mainly because the pleura is a common site for metastasis and reactive, benign changes observed in the pleural space may be confused with MPM [6]. At the same time, prognosis is poor since MPM therapeutic management depends on patient performance status, which is usually not good due to late diagnosis, and is potentially effective mostly in the epitheliod subtype [7]. For these reasons, the availability of effective bio markers is necessary for three clinical aspects of MPM: Early diagnosis, prognosis, and treatment outcome prediction [8].

Aberrant inflammation that could occur during wound healing has been linked to the pathogenesis of a variety of malignancies [9,10]. Environmental and infectious agents are considered key players during carcinogenesis development as they conduce to tissue damage and inflammatory reactions [9]. In the case of MPM, asbestos-induced chronic inflammation—mainly due to the production of reactive oxygen/nitrogen species—results in decreased tumor immunity [11]. Location and inflammatory response type impact on the overall prognosis of MPM patients [9].

PMCs hold a central role in the initiation and resolution of serosal inflammation and repair by secreting various pro- and anti- inflammatory mediators along with immunomodulatory ones [12,13]. It is worth noting that mesothelial regeneration of injured mesothelial surfaces appears diffusely across the traumatized area in contrast to epithelial-like surfaces, in which healing occurs solely from the wound edges [12]. Mesothelial injury and impaired healing can lead to the development of pleural effusions, serosal adhesions, and malignant mesothelioma [13,14]. Several studies have confirmed that following damage, mesothelial cells undergo mesothelial-to-mesenchymal transition (MMT), a process similar to epithelial-to-mesenchymal transition (EMT) [15]. It has been reported that the aggressiveness of MPM may be explained by its partial fibroblastic phenotype in the context of EMT conferring both high invasiveness and chemoresistance [16].

Although the above observations highlight the importance of normal serosal repair following injury, a thorough investigation of the exact role of wound-healing-associated genes in MPM development has not been performed [15]. Research in this direction is even more imperative nowadays due to the wide use of nanoparticles in a variety of applications since nano-sized fibrous particulates have similar properties to asbestos thus raising safety concerns for human health [17,18].

Here, we aimed at the identification of the differential expression of wound-healing-associated genes in MPM. For this purpose, we used established data mining techniques and transcriptomic analysis [19–22]. Moreover, we investigated their potential prognostic value as well as the functional enrichments of gene ontologies (GO) relative to the microRNAs (miRNAs) that regulate the significantly differentially expressed wound-healing-related genes in MPM.

2. Materials and Methods

2.1. Transcriptomic Analysis of Wound-Healing-Associated Genes in MPM

The Oncomine Cancer Microarray database Premium Research Edition (http://www.oncomine.org) was used to investigate the expression profile of wound-healing-associated genes in MPM compared with healthy controls. Gene expression data from the GDS1220 dataset of GEO Profiles were used in which the Affymetrix Human Genome U133A array was used assessing 12,624 genes [23]. We analyzed available data for 82 wound-healing-related genes (from the according list of genes included in the Wound Healing RT^2 Profiler PCR Arrays from Qiagen) that were assessed in the GDS1220 study (Table 1), so as to detect gene expression differences between MPM specimens and healthy controls [23]. The raw data were downloaded in Excel format from Oncomine and only the ones referring to surgically

excised samples were selected, leading to the use of *n* = 40 MPM cases and *n* = 9 controls (*n* = 5 pleura and *n* = 4 lung samples). The gene expression data were log transformed, median centered per array, and the standard deviation was normalized to one per array as described previously [24].

Table 1. The wound-healing-associated genes investigated in this study.

Hugo Gene Nomenclature Committee Gene Name.	Gene Description
ITGA3	Integrin Subunit Alpha 3
ITGAV	Integrin Subunit Alpha V
ITGB6	Integrin Subunit Beta 6
RAC1	Ras-Related C3 Botulinum Toxin Substrate 1 (Rho Family, Small GTP Binding Protein Rac1)
COL5A1	Collagen Type V Alpha 1 Chain
COL5A2	Collagen Type V Alpha 2 Chain
ANGPT1	Angiopoietin 1
COL1A1	Collagen Type I Alpha 1 Chain
COL3A1	Collagen Type III Alpha 1 Chain
CSF3	Colony Stimulating Factor 3
HBEGF	Heparin Binding EGF Like Growth Factor
MIF	Macrophage Migration Inhibitory Factor (Glycosylation-Inhibiting Factor)
TGFA	Transforming Growth Factor Alpha
TNF	Tumor Necrosis Factor
VTN	Vitronectin
CXCL2	C-X-C Motif Chemokine Ligand 2
CXCL5	C-X-C Motif Chemokine Ligand 5
IL6	Interleukin 6
IL10	Interleukin 10
PTGS2	Prostaglandin-Endoperoxide Synthase 2
MAPK3	Mitogen-Activated Protein Kinase 3
PTEN	Phosphatase And Tensin Homolog
IL6ST	Interleukin 6 Signal Transducer
STAT3	Signal Transducer And Activator Of Transcription 3
TGFBR3	Transforming Growth Factor Beta Receptor 3
CTSG	Cathepsin G
F3	Coagulation Factor III, Tissue Factor
F13A1	Coagulation Factor XIII A Chain
PLAUR	Plasminogen Activator, Urokinase Receptor
PLG	Plasminogen
SERPINE1	Serpin Family E Member 1
TIMP1	IMP Metallopeptidase Inhibitor 1
COL1A2	Collagen Type I Alpha 2 Chain
ITGB3	Integrin Subunit Beta 3
ITGB5	Integrin Subunit Beta 5
COL5A3	Collagen Type V Alpha 3 Chain
VEGFA	Vascular Endothelial Growth Factor A
WNT5A	Wnt Family Member 5A
WISP1	WNT1 Inducible Signaling Pathway Protein 1
CTNNB1	Catenin Beta 1
MAPK1	Mitogen-Activated Protein Kinase 1
EGFR	Epidermal Growth Factor Receptor
TGFB1	Transforming Growth Factor Beta 1
CDH1	Cadherin 1
ITGA1	Integrin Subunit Alpha 1
ITGA2	Integrin Subunit Alpha 2
ITGA4	Integrin Subunit Alpha 4
ITGA5	Integrin Subunit Alpha 5
ITGA6	Integrin Subunit Alpha 6
ITGB1	Integrin Subunit Beta 1

Table 1. *Cont.*

Hugo Gene Nomenclature Committee Gene Name.	Gene Description
ACTA2	Actin, Alpha 2, Smooth Muscle, Aorta
ACTA1	Actin, Alpha 1, Skeletal Muscle
RHOA	Ras Homolog Family Member A
TAGLN	Transgelin
COL4A1	Collagen Type IV Alpha 1 Chain
COL4A3	Collagen Type IV Alpha 3 Chain
COL14A1	Collagen Type XIV Alpha 1 Chain
CTSK	Cathepsin K
CTSL2	cathepsin L2
FGA	Fibrinogen Alpha Chain
MMP1	Matrix Metallopeptidase 1
MMP2	Matrix Metallopeptidase 2
MMP7	Matrix Metallopeptidase 7
MMP9	Matrix Metallopeptidase 9
PLAT	Plasminogen Activator, Tissue Type
PLAU	Plasminogen Activator, Urokinase
CSF2	Colony Stimulating Factor 2
CTGF	Connective Tissue Growth Factor
EGF	Epidermal Growth Factor
FGF2	Fibroblast Growth Factor 2
FGF7	Fibroblast Growth Factor 7
HGF	Hepatocyte Growth Factor
IGF1	Insulin Like Growth Factor 1
PDGFA	Platelet Derived Growth Factor Subunit A
CCL2	C-C Motif Chemokine Ligand 2
CCL7	C-C Motif Chemokine Ligand 7
CD40LG	CD40 Ligand
CXCL1	C-X-C Motif Chemokine Ligand 1
CXCL11	C-X-C Motif Chemokine Ligand 11
IL1B	Interleukin 1 Beta
IL2	Interleukin 2
IL4	Interleukin 4

2.2. Evaluation of the Significantly Differentially Expressed Wound-Healing-Related Genes for Prognostic Relevance

We investigated the prognostic relevance of the significantly differentially expressed wound-healing-related genes by creating survival curves, using the publicly available survival data of each patient from the GDS1220 study. Patients were grouped as high expressing (above median) and low expressing (below median) per each significantly differentially expressed gene based on the median value of gene expression. To further evaluate the prognostic significance of the genes that were identified in the analysis of the GDS1220 mesothelioma study, we constructed survival curves from data derived from The Cancer Genome Atlas (TCGA). For this analysis, we used the PROGgeneV2 Prognostic Database software following the same approach used previously [25].

2.3. Functional Annotation Enrichment Gene Ontology Analysis of the miRNAs That Regulate the Significantly Differentially Expressed Wound-Healing-Related Genes in MPM

Functional annotation enrichment analysis of GO relative to Biological Functions and miRNAs was performed, assuming the statistical background of the whole genome. The complete list of the significantly differentially expressed wound-healing-related genes was introduced to the portal ToppFun, an application of the ToppGene Suite (https://toppgene.cchmc.org/). ToppFun reports functional enrichment of input gene lists based on transcriptome (gene expression), proteome (protein domains and interactions), regulome (transcription factor binding sites and miRNA), ontologies (GO, pathway), phenotype (human disease and mouse phenotype), pharmacome (drug–gene associations), and bibliome

(literature co-citation) [26]. Functional enrichments are provided by the ToppFun algorithm, which employs hypergeometric distribution with multiple correction testing (false discovery rate; FDR) to determine statistical significance. Analysis was performed during February 2019.

2.4. Statistical Analysis

The results were analyzed using GraphPad Prism 8.0 (GraphPad Software, San Diego, CA) and R 3.3.2 [27]. Data distribution was tested by the Kolmogorov–Smirnov normality test. Comparisons of gene expressions were performed with the one-tailed t-test for parametric data and the Mann–Whitney U-test for nonparametric data. The Benjamini–Hochberg FDR was employed for multiple correction testing, which reports FDR (or q-value), in order to corroborate the validity of the results. The calculation of the q statistic was based on the formula Q = P value × total number of genes/P-value rank [24]. Statistical significance was set at the $q < 0.05$ level. Kaplan–Meier survival curves were generated using the overall survival data of the MPM patients and by grouping them into high and low gene expressions based on the median. The log-rank (Mantel–Cox) test, which gives equal weight to deaths at all time points, was used. Differences were deemed significant with a $p \leq 0.05$. A multivariate regression was performed using the initial dataset of 30 differentially expressed genes where the ITGAV gene expression was chosen as the dependent variable. At first, all predictors were considered, and a model was derived. This mode had an acceptable R2 value but had to be discarded since the predictors were over-fit. Next, a backwards method was implemented that takes into consideration the Variance Inflation Factor (VIF) value of each predictor. If VIF of an independent variable exceeded the predetermined threshold value of 5, that predictor was discarded from the model. Thus, one avoids multi-collinearity in a model but may still obtain an overfitted model. To avoid this, an additional backwards step-wise regression was performed on the surviving variable so as to have a robust final model.

3. Results

3.1. Identification of the Differential Transcriptional Expression Of Wound-Healing-Associated Genes in MPM

Out of the 82 wound-healing-related genes analyzed, 30 were found significantly differentially expressed in MPM (14 up-regulated/16 down-regulated, results summarized in Table 2). Ten genes (ITGB3, ITGB5, COL5A3, VEGFA, WNT5A, WISP1, CTNNB1, F13A1, PLAUR, TIMP1) were found significantly deregulated in the initial mean value comparison test ($p = 0.008$, $p = 0.023$, $p = 0.016$, $p = 0.0115$, $p = 0.0205$, $p = 0.0055$, $p = 0.024$, $p = 0.0445$, $p = 0.0405$, $p = 0.046$, respectively) but not after the multiple correction testing ($q = 0.055$, $q = 0.1649$, $q = 0,128$, $q = 0.1905$, $q = 0.314$, $q = 0.055$, $q = 0.133$, $q = 0.1898$, $q = 0.1789$, $q = 0.1375$, respectively).

Table 2. Wound-healing-associated genes differentially expressed in malignant pleural mesothelioma (MPM) patients.

	Q Value	FC
	Up-Regulated	
ITGA3	*0.0075*	*3.65983*
ITGAV	*0.019*	*1.62136*
RAC1	*0.0075*	*1.437*
COL5A1	1.29×10^{-3}	*3.4584*
COL5A2	1.06×10^{-3}	*3.7013*
COL1A1	1.24×10^{-3}	*2.6257*
COL3A1	2.79×10^{-3}	*4.0285*
MIF	8.36×10^{-3}	*2.8341*
VTN	4.55×10^{-3}	*7.1654*
MAPK3	1.24×10^{-3}	*2.4605*
IL6ST	*0.0149*	*1.6038*
STAT3	2.51×10^{-3}	*2.9051*

Table 2. *Cont.*

	Q Value	FC
SERPINE1	*0.02*	*3.1149*
COL1A2	*0.0255*	*2.7937*
Down-Regulated		
ITGB6	9.76×10^{-4}	*−2.5496*
ANGPT1	*0.011*	*−2.3463*
CSF3	*0.012*	*−3.5254*
HBEGF	*0.02*	*−1.5826*
TGFA	*0.0126*	*−1.4865*
TNF	*0.04208*	*−4.0594*
CXCL2	3.86×10^{-3}	*−4.6691*
CXCL5	8.40×10^{-4}	*−2.1452*
IL6	*0.01932*	*−6.2047*
IL10	*0.039*	*−1.3583*
PTGS2	7.29×10^{-4}	*−4.408*
PTEN	*0.033*	*−1.407*
TGFBR3	2.14×10^{-3}	*−2.0823*
CTSG	2.08×10^{-3}	*−2.5715*
F3	*0.03*	*−2.3331*
PLG	*0.027*	*−1.5597*

3.2. Prognostic Significance of ITGAV Gene Expression in MPM

Kaplan–Meier analysis of the significantly deregulated wound-healing-related genes in MPM identified the ITGAV gene expression as a predictor of overall survival. Graphical representation of the ITGAV gene expression from the GDS1220 study is shown in Figure 1A. In the GDS1220 study, MPM patients with low ITGAV expression had a median overall survival of 15.7 months versus 12 months of those that had high expression ($p = 0.0263$) (Figure 1B). Analysis from the TCGA patient data derived from the PROGgeneV2 database corroborates that low ITGAV gene expression favors survival in MPM patients ($p = 0.001$) (Figure 2).
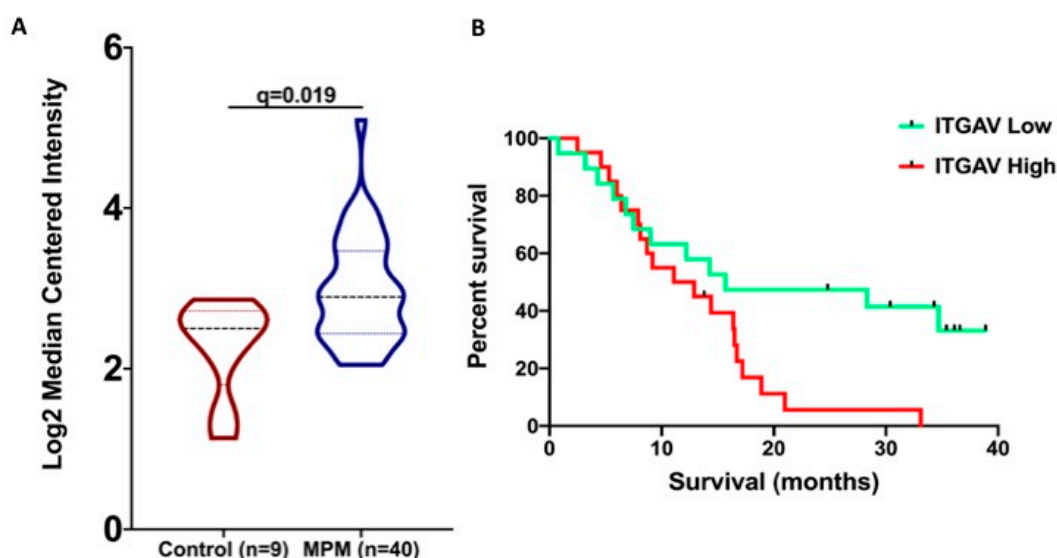

Figure 1. (**A**) Violin plot of the *ITGAV* gene expression shows that it is significantly overexpressed in MPM patients compared to controls. (**B**) Low ITGAV gene expression in MPM patients favors their survival (shown in months).
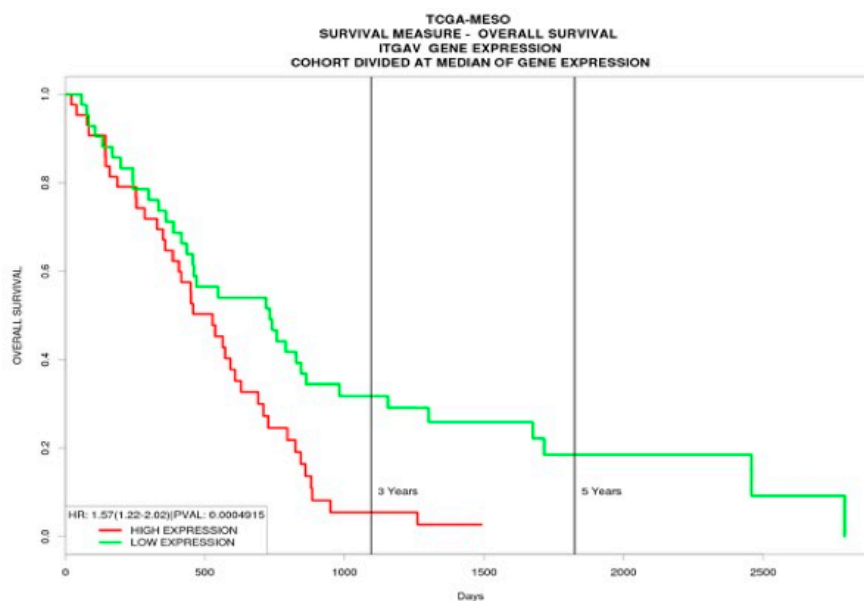
Figure 2. Results of Kaplan–Meier survival analysis from The Cancer Genome Atlas (TCGA) mesothelioma dataset derived from PROGgeneV2 database, shows that low ITGAV gene expression favors survival (shown in days) in MPM patients.

3.3. Statistical Modeling Reveals A Positive Correlation of ITGAV and COL5A1 Gene Expressions

Multivariate regression was performed as shown in Table 3, and the following model was obtained using backwards selection methods:

$$ITGAV = 1.89725 + 0.41537 \; COL5A1 \tag{1}$$

Table 3. Statistical modeling of the correlation of ITGAV and COL5A1 gene expressions.

Coefficients	Estimate	Std. Error	T Value	Pr (>|t|)
(Intercept)	1.89725	0.20885	9.084	4.59×10^{-11} ***
COL5A1	0.41537	0.07451	5.574	2.18×10^{-6} ***

The model explains the 43.54% (adjusted R^2 = 0.4354) of the variability of the response data around its mean. F-statistic and *p*-value indicate that the model is significant for the explanation of the variability of the response data. The coefficients of the model are positive, hence whenever the value of COL5A1 increases, the same happens to the value of ITGAV. The value of each coefficient shows the increase of the value of ITGAV if the corresponding variable is increased or decreased by one unit, while the rest remain fixed.

3.4. Enriched Gene Ontologies (GO) Relative To Regulating miRNAs of the Significantly Differentially Expressed Wound-Healing-Associated Genes In MPM

The complete set of the significantly differentially expressed wound-healing-associated genes was entered in the ToppFun software. The top five enriched GO for biological functions are presented in Table 4, and the miRNAs that regulate the differentially expressed genes are shown in Table 5.

Table 4. Functional enrichment analysis relative to Biological Functions of the wound-healing-associated genes differentially expressed in MPM patients *.

	ID	Name	P-Value	FDR B&H	FDR B&Y	Bonferroni	Genes From Input	Genes in Annotation
1	GO:0040011	locomotion	2.531×10^{-23}	7.177×10^{-20}	6.120×10^{-19}	7.177×10^{-20}	26	1735
2	GO:0016477	cell migration	5.798×10^{-23}	1.644×10^{-19}	24	1300		
3	GO:0051674	localization of cell	5.395×10^{-22}	3.825×10^{-19}	3.262×10^{-18}	1.530×10^{-18}	24	1428
4	GO:0048870	cell motility	5.395×10^{-22}	3.825×10^{-19}	3.262×10^{-18}	1.530×10^{-18}	24	1428
5	GO:0030334	regulation of cell migration	1.635×10^{-21}	9.274×10^{-19}	7.909×10^{-18}	4.637×10^{-18}	20	742

* Results were obtained through ToppFun, an application of the ToppGene suite (https://toppgene.cchmc.org/). FDR: False discovery rate; B&H: Benjamini–Hochberg; B&Y: Benjamini–Yekutieli. Only the top five results are presented.

Table 5. Functional enrichment analysis relative to miRNAs of the wound-healing-associated genes differentially expressed in MPM patients *.

	ID	Name	Source	P-Value	FDR B&H	FDR B&Y	Bonferroni	Genes From Input	Genes in Annotation
1	hsa-miR-143-3p:Functional MTI	Functional MTI	miRTarbase	5.442×10^{-12}	1.459×10^{-8}	1.236×10^{-7}	1.459×10^{-8}	7	228
2	hsa-miR-223-3p:Functional MTI	Functional MTI	miRTarbase	5.747×10^{-10}	7.704×10^{-7}	6.526×10^{-6}	1.541×10^{-6}	5	98
3	hsa-miR-29b-3p:Functional MTI	Functional MTI	miRTarbase	1.159×10^{-9}	1.036×10^{-6}	8.776×10^{-6}	3.108×10^{-6}	6	261
4	hsa-miR-29a:PITA	hsa-miR-29a:PITA TOP	PITA	3.728×10^{-9}	1.666×10^{-6}	1.411×10^{-5}	9.995×10^{-6}	7	583
5	hsa-miR-29c:PITA	hsa-miR-29c:PITA TOP	PITA	3.728×10^{-9}	1.666×10^{-6}	1.411×10^{-5}	9.995×10^{-6}	7	583

* Results were obtained through ToppFun, an application of the ToppGene suite (https://toppgene.cchmc.org/). FDR: False discovery rate; B&H: Benjamini–Hochberg; B&Y: Benjamini–Yekutieli. Only the top five results are presented.

4. Discussion

Chronic tissue repair and insistent immune system stimulation following the accumulation of inhaled asbestos fibers in the pleural space are key oncogenic processes during MPM development [28]. In this study, we used transcriptome data mining in order to assess the differential mRNA expression of wound-healing-related genes in MPM. We analyzed available data for 82 genes, of which 30 were found significantly deregulated in MPM specimens compared with healthy tissues. Identified genes are mainly involved in inflammation (CXCL2, CXCL5, IL6, IL10), cellular adhesion (ITGA3, ITGAV, ITGB6), tissue remodeling (CTSG, F3, PLG, SERPINE1), and extracellular matrix organization (COL1A1, COL3A1, COL5A1, COL5A2, CSF3, HBEGF, MIF, TGFA, VTN), fundamental processes in the induction of EMT and cancer progression [29–32]. A recent study has suggested that asbestos induces mesothelial-to-fibroblastic transition in an inflammasome-dependent manner and this seems to apply for other pathogenic particles as well [28,33,34].

The acquisition of a mesenchymal phenotype by PMCs has been correlated with the sarcomatoid histological type of MPM, the latter being associated to worse prognosis [16,35]. It has been suggested that in MPM patients with sarcomatoid histology, radical surgery should be excluded, and therapy should aim at symptom control and preservation of quality of life [36]. Considering the importance of clear histological subtype distinction in the initiation of the appropriate therapeutic intervention, it would be of great interest to investigate the transcriptional expression of the 30 significantly deregulated genes—identified in this study—with respect to the MPM phenotype [22]. Unfortunately, data relative to the histological subtype of MPM specimens were not available in the GDS1220 mesothelioma study.

Among the 30 significantly differentially expressed wound-healing-associated genes in MPM, ITGAV was identified as a predictor of overall survival in patients suffering from this type of cancer. In the transcriptomic analysis, ITGAV was found significantly up-regulated in MPM subjects compared with healthy controls, and survival analysis revealed that low ITGAV gene expression favors the survival of MPM patients. In accordance with our results, recent studies have reported the tumor-promoting effect of ITGAV via the furtherance of the EMT process [37,38]. The gene expression level of the ITGAV integrin has also been associated with global survival in patients with colorectal cancer, both in univariate and multivariate analyses [39].

Following the above findings, our regression modelling predicted a significant positive correlation in the expression profiles of the ITGAV and COL5A1 genes. The latter encodes the a1 chain of type V collagen, a fibril-forming collagen that is mainly distributed in the lung, cornea, bone, and fetal membranes, together with type I collagen [40,41]. Interestingly, COL5A1 has been included in a 10-gene signature that is associated with poor survival both in patients with high-grade serous ovarian cancer and renal cell carcinoma [42,43].

Finally, the biological functions mediated by the differentially regulated genes as revealed by the GO functional enrichment analysis were pertinent to wound healing functions, such as cell locomotion, mobility, and migration. Furthermore, the GO annotation enrichment analysis predicted that the 30 wound-healing-related genes that were found significantly deregulated in MPM might be targets of the hsa-miR-143, hsa-miR-223, and the hsa-miR-29 miRNA family members. MicroRNAs have emerged as significant players in the biology of MPM, whilst miRNA-based therapy for the treatment of MPM has been suggested as an exciting area of research [44]. The hsa-miR-29c has been identified as an epigenetic regulator in MPM via the down-regulation of DNA methyltransferases and the up-regulation of demethylating genes [45]. In addition, increased expression of this miRNA has been linked to a more favorable prognosis in MPM [45]. On the other hand, hsa-miR-143 has been linked to MPM only once, in a study that showed that its expression is significantly reduced in MPM as compared to non-neoplastic corresponding tissue [46]. Its functional role in MPM is unknown, however in other cancers, the decreased expression of has-miR-143 has been shown to promote EMT, tumor growth, and metastasis [47,48]. Overall, these reports strengthen the findings of our in silico transcriptomic analysis implicating 30 wound-healing-associated genes in MPM pathogenicity.

However, it is imperative to investigate the transcriptional expression of these genes in the clinical setting, taking into account both MPM phenotype and history of asbestos exposure.

5. Conclusions

Conclusively, using data mining and transcriptomic analysis, we have identified a significant deregulation of 30 wound-healing-related genes in MPM specimens compared to healthy tissues. We have also demonstrated that these genes are possible targets of the hsa-miR-143, hsa-miR-223, and the hsa-miR-29 miRNA family members, which contribute in MPM pathobiology as evidenced by recent studies. Finally, we have identified ITGAV as a novel predictor of overall survival in MPM. Our results highlight the role of impaired tissue repair in MPM development and should be further validated experimentally.

References

1. Nasreen, N.; Mohammed, K.A.; Mubarak, K.K.; Baz, M.A.; Akindipe, O.A.; Fernandez-Bussy, S.; Antony, V.B. Pleural mesothelial cell transformation into myofibroblasts and haptotactic migration in response to TGF-β1 in vitro. *Am. J. Physiol. Cell. Mol. Physiol.* **2009**, *297*, L115–L124. [CrossRef] [PubMed]
2. Carbone, M.; Yang, H. Molecular pathways: Targeting mechanisms of asbestos and erionite carcinogenesis in mesothelioma. *Clin. Cancer. Res.* **2012**, *18*, 598–604. [CrossRef] [PubMed]
3. Carbone, M.; Ly, B.H.; Dodson, R.F.; Pagano, I.; Morris, P.T.; Dogan, U.A.; Gazdar, A.F.; Pass, H.I.; Yang, H. Malignant mesothelioma: Facts, Myths, and Hypotheses. *J. Cell. Physiol.* **2012**, *227*, 44–58. [CrossRef]
4. Sinis, S.I.; Hatzoglou, C.; Gourgoulianis, K.I.; Zarogiannis, S.G. Carbon Nanotubes and Other Engineered Nanoparticles Induced Pathophysiology on Mesothelial Cells and Mesothelial Membranes. *Front. Physiol.* **2018**, *9*, 295. [CrossRef] [PubMed]
5. Schultze, F.; Gao, X.; Virzonis, D.; Damiati, S.; Schneider, M.R.; Kodzius, R. Air quality effects on human healthand approaches for its assessment through microfluidic chips. *Genes* **2017**, *8*, 10.
6. Baas, P.; Fennel, D.; Kerr, K.M.; Van Scil, P.E.; Haas, R.L.; Peters, S.; ESMO Guidelines Committee. Malignant pleural mesothelioma: ESMO Clinical Practice Guidelines for diagnosis, treatment and follow-up. *Ann. Oncol.* **2015**, *26*, 31–39. [CrossRef]
7. Imperatori, A.S.; Castiglioni, M.; Mortara, L.; Nardecchia, E.; Rotolo, N. The challenge of prognostic markers in pleural mesothelioma. *J. Thorac. Dis.* **2013**, *5*, 205–206. [PubMed]
8. Greillier, L.; Baas, P.; Welch, J.J.; Hasan, B.; Passioukov, A. Biomarkers for malignant pleural mesothelioma: Current status. *Mol. Diagn. Ther.* **2008**, *12*, 375–390. [CrossRef]
9. Linton, A.; Van Zandwijk, N.; Reid, G.; Clarke, S.; Cao, C.; Kao, S. Inflammation in malignant mesothelioma–friend or foe? *Ann. Cardiothorac. Surg.* **2012**, *1*, 516–522.
10. Arnold, K.M.; Opdenaker, L.M.; Flynn, D.; Sims-Mourtada, J. Wound Healing and Cancer Stem Cells: Inflammation as a Driver of Treatment Resistance in Breast Cancer. *Cancer Growth Metastasis* **2015**, *8*, 1–13. [CrossRef]
11. Matsuzaki, H.; Maeda, M.; Lee, S.; Nishimura, Y.; Kumagai-Takei, N.; Hayashi, H.; Yamamoto, S.; Hatayama, T.; Kojima, Y.; Tabata, R.; et al. Asbestos-Induced Cellular and Molecular Alteration of Immunocompetent Cells and Their Relationship with Chronic Inflammation and Carcinogenesis. *J. Biomed. Biotechnol.* **2012**, *2012*, 1–9. [CrossRef] [PubMed]
12. Mutsaers, S.E. The mesothelial cell. *Int. J. Biochem. Cell. Biol.* **2004**, *36*, 9–16. [CrossRef]
13. Mutsaers, S.E.; Wilkosz, S. Structure and Function of Mesothelial Cells. *Periton. Carcinomat.* **2007**, *134*, 1–19.

14. Nagai, H.; Chew, S.H.; Okazaki, Y.; Funahashi, S.; Namba, T.; Kato, T.; Enomoto, A.; Jiang, L.; Akatsuka, S.; Toyokuni, S. Metamorphosis of mesothelial cells with active horizontal motility in tissue culture. *Sci. Rep.* **2013**, *3*, 1144. [CrossRef] [PubMed]

15. Mutsaers, S.E.; Birnie, K.; Lansley, S.; Herrick, S.E.; Lim, C.-B.; Prele, C.M.; PrêLe, C.M. Mesothelial cells in tissue repair and fibrosis. *Front. Pharmacol.* **2015**, *6*, 113. [CrossRef]

16. Schramm, A.; Opitz, I.; Thies, S.; Seifert, B.; Moch, H.; Weder, W.; Soltermann, A. Prognostic significance of epithelial–mesenchymal transition in malignant pleural mesothelioma. *Eur. J. Cardio-Thoracic Surg.* **2010**, *37*, 566–572. [CrossRef] [PubMed]

17. Jaurand, M.-C.F.; Renier, A.; Daubriac, J. Mesothelioma: Do asbestos and carbon nanotubes pose the same health risk? *Part. Fibre Toxicol.* **2009**, *6*, 16. [CrossRef] [PubMed]

18. Nagai, H.; Toyokuni, S. Biopersistent fiber-induced inflammation and carcinogenesis: Lessons learned from asbestos toward safety of fibrous nanomaterials. *Arch. Biochem. Biophys.* **2010**, *502*, 1–7. [CrossRef]

19. Jagirdar, R.; Solenov, E.I.; Hatzoglou, C.; Molyvdas, P.-A.; Gourgoulianis, K.I.; Zarogiannis, S.G. Gene expression profile of aquaporin 1 and associated interactors in malignant pleural mesothelioma. *Gene* **2013**, *517*, 99–105. [CrossRef]

20. Tasiopoulou, V.; Magouliotis, D.; Solenov, E.I.; Vavougios, G.; Molyvdas, P.-A.; Gourgoulianis, K.I.; Hatzoglou, C.; Zarogiannis, S.G. Transcriptional over-expression of chloride intracellular channels 3 and 4 in malignant pleural mesothelioma. *Comput. Boil. Chem.* **2015**, *59*, 111–116. [CrossRef]

21. Vavougios, G.D.; I Solenov, E.; Hatzoglou, C.; Baturina, G.S.; E Katkova, L.; Molyvdas, P.A.; Gourgoulianis, K.I.; Zarogiannis, S.G. Computational genomic analysis of PARK7 interactome reveals high BBS1 gene expression as a prognostic factor favoring survival in malignant pleural mesothelioma. *Am. J. Physiol. Cell. Mol. Physiol.* **2015**, *309*, 677–686. [CrossRef] [PubMed]

22. Rouka, E.; Vavougios, G.D.; Solenov, E.I.; Gourgoulianis, K.I.; Hatzoglou, C.; Zarogiannis, S.G. Transcriptomic Analysis of the Claudin Interactome in Malignant Pleural Mesothelioma: Evaluation of the Effect of Disease Phenotype, Asbestos Exposure, and CDKN2A Deletion Status. *Front. Physiol.* **2017**, *8*, 4969. [CrossRef] [PubMed]

23. Gordon, G.J.; Rockwell, G.N.; Jensen, R.V.; Rheinwald, J.G.; Glickman, J.N.; Aronson, J.P.; Pottorf, B.J.; Nitz, M.D.; Richards, W.G.; Sugarbaker, D.J.; et al. Identification of Novel Candidate Oncogenes and Tumor Suppressors in Malignant Pleural Mesothelioma Using Large-Scale Transcriptional Profiling. *Am. J. Pathol.* **2005**, *166*, 1827–1840. [CrossRef]

24. Rhodes, D.R.; Yu, J.; Shanker, K.; Deshpande, N.; Varambally, R.; Ghosh, D.; Barrette, T.; Pander, A.; Chinnaiyan, A.M. ONCOMINE: A Cancer Microarray Database and Integrated Data-Mining Platform. *Neoplasia* **2004**, *6*, 1–6. [CrossRef]

25. Goswami, C.P.; Nakshatri, H. PROGgeneV2: Enhancements on the existing database. *BMC Cancer* **2014**, *14*, 970. [CrossRef] [PubMed]

26. Chen, J.; Bardes, E.E.; Aronow, B.J.; Jegga, A.G. ToppGene Suite for gene list enrichment analysis and candidate gene prioritization. *Nucleic Acids Res.* **2009**, *37*, W305–W311. [CrossRef] [PubMed]

27. R Core Team. R: A Language and Environment for Statistical Computing. R Foundation for Statistical Computing: Vienna, Austria, 2013. Available online: http://www.R-project.org/ (accessed on 20 May 2018).

28. Frei, C.; Opitz, I.; Soltermann, A.; Fischer, B.; Moura, U.; Rehrauer, H.; Weder, W.; Stahel, R.; Felley-Bosco, E. Pleural mesothelioma side populations have a precursor phenotype. *Carcinogenesis* **2011**, *32*, 1324–1332. [CrossRef]

29. López-Novoa, J.M.; Nieto, M.A. Inflammation and EMT: An alliance towards organ fibrosis and cancer progression. *EMBO Mol. Med.* **2009**, *1*, 303–314. [CrossRef]

30. Makrilia, N.; Kollias, A.; Manolopoulos, L.; Syrigos, K. Cell Adhesion Molecules: Role and Clinical Significance in Cancer. *Cancer Investig.* **2009**, *27*, 1023–1037. [CrossRef]

31. Lu, P.; Weaver, V.M.; Werb, Z. The extracellular matrix: A dynamic niche in cancer progression. *J. Cell. Biol.* **2012**, *196*, 395–406. [CrossRef]

32. Pickup, M.W.; Mouw, J.K.; Weaver, V.M. The extracellular matrix modulates the hallmarks of cancer. *EMBO Rep.* **2014**, *15*, 1243–1253. [CrossRef] [PubMed]

33. Thompson, J.K.; MacPherson, M.B.; Beuschel, S.L.; Shukla, A. Asbestos-Induced Mesothelial to Fibroblastic Transition Is Modulated by the Inflammasome. *Am. J. Pathol.* **2017**, *187*, 665–678. [CrossRef] [PubMed]

34. Sayan, M.; Mossman, B.T. The NLRP3 inflammasome in pathogenic particle and fibre-associated lung inflammation and diseases. *Part. Fibre Toxicol.* **2016**, *13*, 674. [CrossRef] [PubMed]

35. Fassina, A.; Cappellesco, R.; Guzzardo, V.; Della Via, L.; Piccolo, S.; Ventura, L.; Fassan, M. Epithelial-mesenchymal transition in malignant mesothelioma. *Mod. Pathol.* **2012**, *25*, 86–99. [CrossRef] [PubMed]

36. Balduyck, B.; Trousse, D.; Nakas, A.; Martin-Ucar, A.E.; Edwards, J.; Waller, D.A. Therapeutic Surgery for Nonepithelioid Malignant Pleural Mesothelioma: Is it Really Worthwhile? *Ann. Thorac. Surg.* **2010**, *89*, 907–911. [CrossRef] [PubMed]

37. Waisberg, J.; Viana, L.D.S.; Junior, R.J.A.; Silva, S.R.M.; Denadai, M.V.A.; Margeotto, F.B.; De Souza, C.S.; Matos, D. Overexpression of the ITGAV gene is associated with progression and spread of colorectal cancer. *Anticancer Res.* **2014**, *34*, 5599–5607. [PubMed]

38. Ding, Y.; Pan, Y.; Liu, S.; Jiang, F.; Jiao, J. Elevation of MiR-9–3p suppresses the epithelial-mesenchymal transition of nasopharyngeal carcinoma cells via down-regulating FN1, ITGB1 and ITGAV. *Cancer Boil. Ther.* **2017**, *18*, 414–424. [CrossRef]

39. Linhares, M.M.; Affonso, R.J.; Viana, L.D.S.; Silva, S.R.M.; Denadai, M.V.A.; De Toledo, S.R.C.; Matos, D. Genetic and Immunohistochemical Expression of Integrins ITGAV, ITGA6, and ITGA3 As Prognostic Factor for Colorectal Cancer: Models for Global and Disease-Free Survival. *PLoS ONE* **2015**, *10*, e0144333. [CrossRef]

40. Zhang, J.J.; Yano, H.; Sasaki, T.; Matsuo, N.; Yoshioka, H. The pro-α1(V) collagen gene (Col5a1) is coordinately regulated by miR-29b with core promoter in cultured cells. *Connect. Tissue Res.* **2018**, *59*, 263–273. [CrossRef]

41. Gelse, K. Collagens—structure, function, and biosynthesis. *Adv. Drug Deliv. Rev.* **2003**, *55*, 1531–1546. [CrossRef]

42. Cheon, D.J.; Tong, Y.; Sim, M.S.; Dering, J.; Berel, D.; Cui, X.; Lester, J.; Beach, J.A.; Tighiouart, M.; Walts, A.E.; et al. A collagen-remodeling gene signature regulated by TGF-β signaling is associated with metastasis and poor survival in serous ovarian cancer. *Clin. Cancer Res.* **2014**, *20*, 711–723. [CrossRef] [PubMed]

43. Boguslawska, J.; Kedzierska, H.; Poplawski, P.; Rybicka, B.; Tanski, Z.; Piekielko-Witkowska, A.; Information, P.E.K.F.C. Expression of Genes Involved in Cellular Adhesion and Extracellular Matrix Remodeling Correlates with Poor Survival of Patients with Renal Cancer. *J. Urol.* **2016**, *195*, 1892–1902. [CrossRef] [PubMed]

44. Reid, G. MicroRNAs in mesothelioma: From tumor suppressors and biomarkers to therapeutic targets. *J. Thorac. Dis.* **2015**, *7*, 1031–1040. [PubMed]

45. Pass, H.I.; Goparaju, C.; Ivanov, S.; Donington, J.; Carbone, M.; Hoshen, M.; Cohen, D.; Chajut, A.; Rosenwald, S.; Dan, J.; et al. has-miR-29c is linked to the prognosis of malignant pleural mesothelioma. *Cancer Res.* **2010**, *70*, 1916–1924. [CrossRef] [PubMed]

46. Andersen, M.; Grauslund, M.; Ravn, J.; Sorensen, J.B.; Andersen, C.B.; Santoni-Rugiu, E. Diagnostic potential of miR126, miR143, miR145, miR-652 in malignant pleural mesothelioma. *J. Mol. Diagn.* **2014**, *16*, 418–430. [CrossRef] [PubMed]

47. He, M.; Zhan, M.; Chen, W.; Xu, S.; Long, M.; Shen, H.; Shi, Y.; Liu, Q.; Mohan, M.; Wang, J. MiR-143-5p Deficiency Triggers EMT and Metastasis by Targeting HIF-1α in Gallbladder Cancer. *Cell. Physiol. Biochem.* **2017**, *42*, 2078–2092. [CrossRef] [PubMed]

48. Zhou, L.; Dong, J.; Huang, G.; Sun, Z.; Wu, J. MicroRNA-143 inhibits cell growth by targeting ERK5 and MAP3K7 in breast cancer. *Braz. J. Med. Boil. Res.* **2017**, *50*, 5891. [CrossRef]